The Radiation Tolerance of Strained Si/SiGe n-MODFETs

Anuj Madan, *Student Member, IEEE*, Bongim Jun, *Member, IEEE*, Ryan M. Diestelhorst, *Student Member, IEEE*, Aravind Appaswamy, *Student Member, IEEE*, John D. Cressler, *Fellow, IEEE*, Ronald D. Schrimpf, *Fellow, IEEE*, Daniel M. Fleetwood, *Fellow, IEEE*, Paul W. Marshall, *Member, IEEE*, Tamara Isaacs-Smith, John R. Williams, and Steven J. Koester, *Senior Member, IEEE*

***Abstract*—The radiation tolerance of strained Si/SiGe n-MODFETs is investigated, using 10 keV X-rays, 63 MeV high energy protons, and 4 MeV low energy protons. The effects of radiation exposure on two major device design parameters (L_{SD} and L_G) in T-gate Si/SiGe n-MODFETs devices are examined. A strong dependence on source-drain spacing is observed for both the DC and RF characteristics. A drift-diffusion TCAD framework is used for 2-D device simulations. We believe that the low energy protons damage the SiGe/strained-Si/SiGe lattice, leading to partial strain relaxation. The conduction band-offset (CBO) of the strained SiGe/Si heterojunction is lowered leading to higher gate current leakage. The presence of radiation-induced bulk traps in the unrelaxed SiGe layers on the device behavior is also investigated.**

***Index Terms*—Bulk traps, buried-channel, displacement damage, MODFET, radiation effects, SiGe, silicon-germanium, strain.**

I. INTRODUCTION

BANDGAP-engineered Si/SiGe n-MODFETs (modulation-doped FETs or HEMTs) are promising candidates for future RF and mixed-signal circuit applications [1], [2]. Their demonstrated mobility advantage at low drain voltage and current levels compared to conventional CMOS makes them very attractive candidates for high speed and low power applications [3]. Currently, impressive levels of device performance (f_{max} of 200 GHz at 70 nm gate lengths) have been achieved, and the buried channel nature of these devices ensures that their noise characteristics are particularly attractive compared to CMOS. The potential compatibility of Si/SiGe MODFETs with traditional silicon-based wafer manufacturing, and the ability to achieve complementary device topologies (n-MODFET + p-MODFET = C-MODFET) on the same silicon wafer [4], [5], differentiates Si/SiGe MODFETs from their III-V counterparts. While the robust radiation tolerance of traditional III-V MODFETs is well-established [6], [7], there are at present no available radiation data on Si/SiGe MODFETs. We report here, the DC and RF performance of Si/SiGe n-MODFETs irradiated with both X-rays and protons. The effects of radiation exposure on two major device design parameters (L_{SD} and L_G) in these T-gate Si/SiGe n-MODFETs devices are examined. The underlying damage mechanisms for displacement damage and trap-generation in unrelaxed SiGe layers of n-MODFETs are also investigated by means of 2-D device simulations.

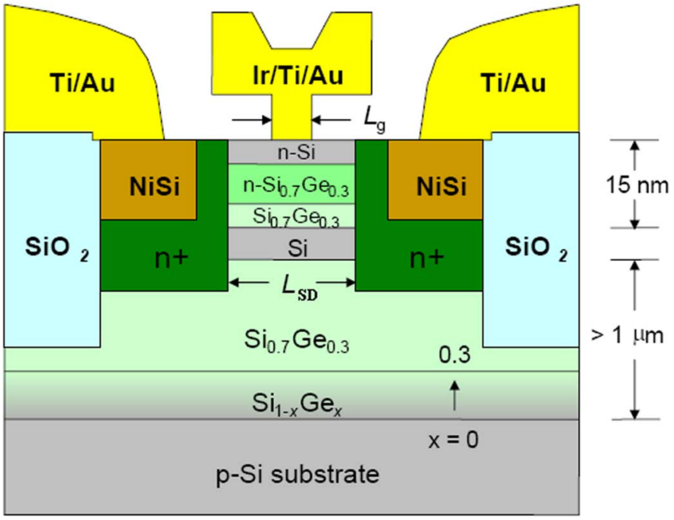

Fig. 1. Cross-section of the Si/SiGe n-MODFET [8].

II. DEVICE TECHNOLOGY

Fig. 1 shows a schematic cross-section of the Si/SiGe n-MODFET investigated [8]. The source-to-drain length (L_{SD}) is defined to be the distance between the source and drain implants. Devices with gate lengths (L_G) ranging between 70 nm to 100 nm, and L_{SD} ranging between 300 nm to 800 nm, were used for our experiments.

A buried silicon channel is formed, enclosed by $Si_{0.7}Ge_{0.3}$ layers on both top and bottom, and the entire channel structure is grown on a step-graded SiGe relaxed buffer layer by ultrahigh vacuum chemical vapor deposition (UHV/CVD). The conduction band offsets at the Si/SiGe interface provide electron confinement for carriers in the silicon channel, as depicted in Fig. 2.

Manuscript received July 21, 2007; revised August 30, 2007. This work was supported by the Defense Threat Reduction Agency under the Radiation Hardened Microelectronics Program, an AFOSR MURI program, NASA-GSFC under the NASA Electronic Parts and Packaging (NEPP) Program, NAVSEA Crane, ATK-Mission Research, IBM, and the Georgia Electronic Design Center at Georgia Tech.

A. Madan, B. Jun, R. M. Diestelhorst, A. Appaswamy, and J. D. Cressler are with the School of Electrical and Computer Engineering, Georgia Institute of Technology, Atlanta, GA 30308 USA (e-mail: madan@ece.gatech.edu).

R. D. Schrimpf and D. M. Fleetwood are with Vanderbilt University, Nashville, TN 37235 USA.

P. W. Marshall is a consultant to NASA-GSFC, Brookneal, VA 24528 USA.

T. Isaacs-Smith, and J. R. Williams are with Auburn University, Auburn, AL 36849USA.

S. J. Koester is with IBM T. J. Watson Research Center, Yorktown Heights, NY 10598 USA.

Color versions of one or more of the figures in this paper are available online at http://ieeexplore.ieee.org.

Digital Object Identifier 10.1109/TNS.2007.907871

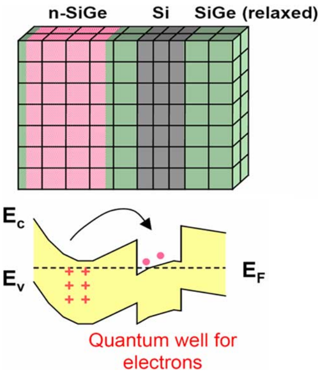

Fig. 2. Silicon layer enclosed between the SiGe layers forms the quantum well channel.

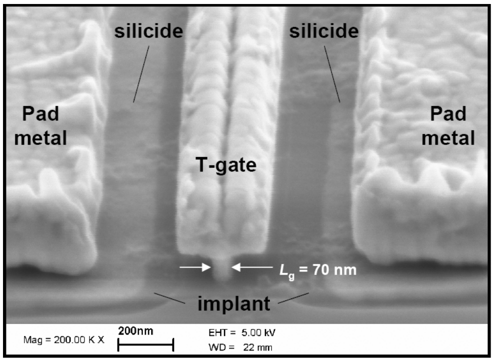

Fig. 3. TEM of a SiGe n-MODFET showing the T-gate structure with $\mathrm{L_G} = 70$ nm and $\mathrm{L_{SD}} = 300$ nm.

The T-shaped Ir/Ti/Au gates were patterned using electron beam lithography. The gate stack was not self-aligned to the source and drain. Fig. 3 shows a TEM image of the Si/SiGe n-MODFET fabricated with a metal T-gate. A more detailed discussion of the device fabrication is given in [8] and for brevity is not repeated here.

III. EXPERIMENTAL DETAILS

The DC characteristics of the devices were measured at room temperature using an Agilent 4155 Semiconductor Parameter Analyzer. Samples were wire-bonded into 28-pin DIP packages, and total ionizing dose radiation tests were performed at room temperature using 10 keV X-rays, at a dose rate of 540 rad($\mathrm{SiO_2}$)/s, to total doses as high as 5.4 Mrad($\mathrm{SiO_2}$). Low-energy proton exposure was also performed at room temperature using a 4 MeV proton beam at The Space Research Institute at Auburn University, at a dose rate of 1 krad($\mathrm{SiO_2}$)/s. The 4 MeV protons were used to better understand the impact of displacement damage on the buried Si/SiGe interfaces within the device. High energy proton exposure was performed at Crocker Nuclear Laboratory at University of California, Davis using a 63 MeV proton beam. A dose rate of 1.1 krad($\mathrm{SiO_2}$)/s was used to expose these devices at room temperature. All terminals were grounded during all exposures. Table I summarizes the experimental test details. The DC characteristics of the devices were measured immediately after each cumulative dose was reached, and additional post-irradiation data were re-measured after approximately 120 hours to assess spontaneous self-annealing. An Agilent 8510C Vector Network Analyzer was used to extract S-parameters and RF metrics, both before and after irradiation (on-wafer RF measurements necessitate unpackaged passive exposure of devices).

TABLE I
RADIATION EXPOSURE DETAILS

Source Beam	Dose Rate ($\mathrm{SiO_2}$/s)	Temperature	Bias
10 keV X-ray	540 rad	Room T	Grounded
4 MeV Proton	1 krad	Room T	Grounded
63 MeV Proton	1.1 krad	Room T	Grounded

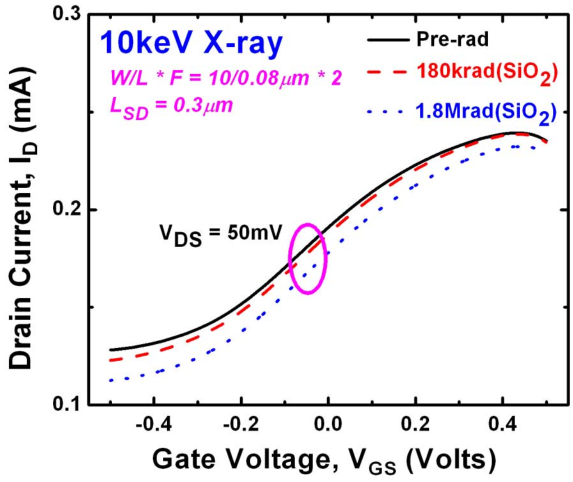

Fig. 4. Impact of 10 keV X-ray irradiation on the transfer characteristics.

IV. EXPERIMENTAL RESULTS

A. DC Characteristics

Fig. 4 shows typical I_D -$\mathrm{V_{GS}}$ transfer characteristics as a function of X-ray dose for a 2-finger Si/SiGe n-MODFET with width and length dimensions of $\mathrm{W/L} = 10/0.08$ and $\mathrm{L_{SD}}$ of 300 nm, after X-ray exposure. The gate current is not appreciably degraded. Fig. 5 shows the output characteristics of a device with $\mathrm{L_{SD}}$ of 600 nm, indicating significant X-ray induced current degradation in saturation. A similar trend in transfer characteristics is observed for 63 MeV proton irradiation of a device with $\mathrm{L_{SD}}$ of 600 nm and $\mathrm{L_G}$ of 80 nm, as shown in Fig 6. The degradation trends are consistent in all the irradiated devices. Fig. 7 shows the impact of low energy proton exposure on the transfer characteristics of a device with similar dimensions (the $\mathrm{V_{DS}}$ bias is different). The degradation behavior of the transfer characteristics induced by the 4 MeV proton irradiation is attributed to the gate current change after irradiation, presumably due to displacement damage (Fig. 7).

Possible proton-induced displacement damage in the unrelaxed $\mathrm{Si_{0.7}}$ Ge $_{0.3}$ layer on top of the silicon channel can also reduce the electron confinement in the channel through strain

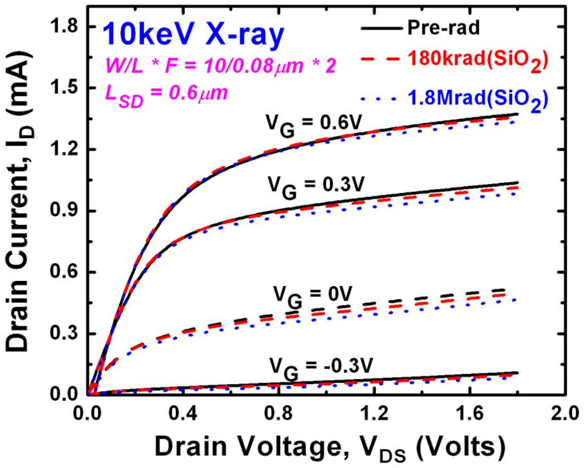

Fig. 5. X-ray radiation impact on output characteristics.

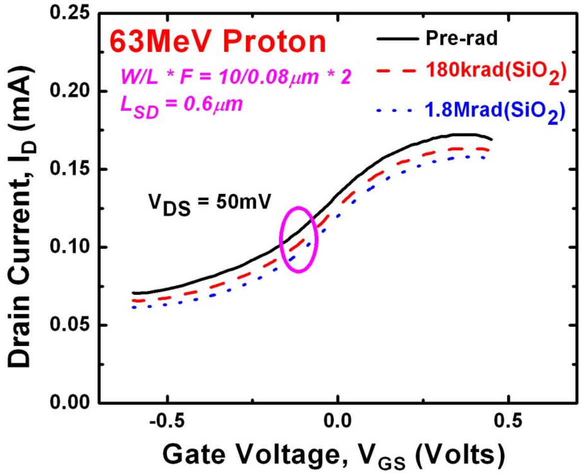

Fig. 6. Impact of 63MeV proton irradiation on transfer characteristics.

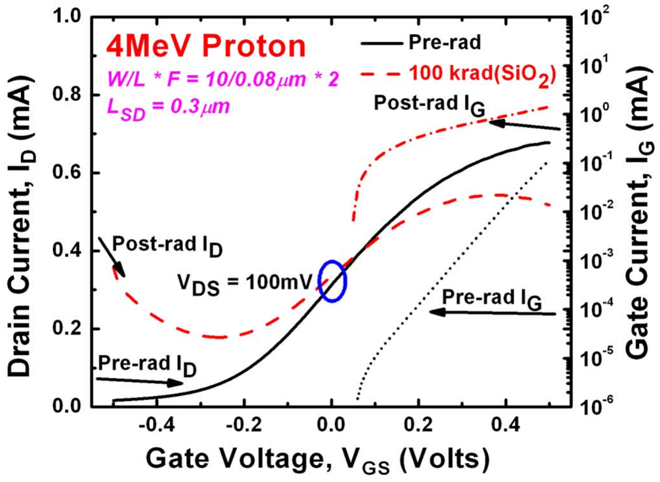

Fig. 7. Impact of 4 MeV proton irradiation on the transfer characteristics.

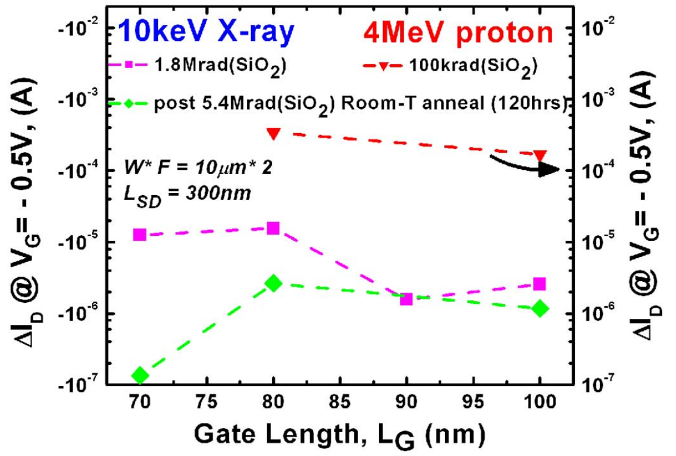

Fig. 8. Impact of irradiation on off-state leakage current as a function of gate length.

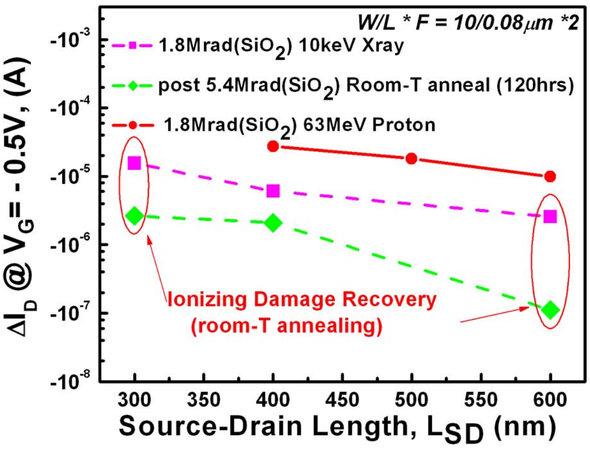

Fig. 9. Variation of the X-ray and 63 MeV proton impact on off-state leakage with $\mathrm{L_{SD}}$.

relaxation, degrading the current drive. The excess off-state leakage current is shown in Fig. 8, and following proton exposure increases with dose, presumably due to displacement damage effects. An interesting *reduction* in leakage current is observed, however, following X-ray exposure (note that the left and right y-axes have different signs). It is interesting that the X-ray irradiation consistently reduces excess off-state leakage at room temperature. Detailed device simulation studies are presented in Section V to investigate the role of traps in Si/SiGe n-MODFETs and establish a correlation with observed radiation damage.

Fig. 9 shows the off-state leakage current degradation as a function of $\mathrm{L_{SD}}$ for devices with a fixed $\mathrm{L_G} = 80$ nm. Observe that the leakage recovery via X-ray exposure is more pronounced in devices with longer $\mathrm{L_{SD}}$. A similar dependence on $\mathrm{L_G}$ and $\mathrm{L_{SD}}$ scaling is observed for the saturated drain current, as shown in Figs. 10 and 11. Low energy protons clearly induce more damage in these devices compared to X-rays, at fixed total dose, suggesting the strong role of displacement damage.

The low field effective mobility (μ_{eff}) was extracted for the devices with $\mathrm{L_{SD}} = 400$ nm and 600 nm, and $(\mathrm{W/L}) * \mathrm{F} = (10/0.08) * 2$ (F is the number of gate fingers), prior to irradiation and as a function of total dose. From the I_D - $\mathrm{V_{GS}}$ and linear transconductance characteristics, the channel mobility was extracted from the slope of the quasi-linear function of $I_D/(g_m)^{1/2}$ vs. V_{GS}, which eliminates

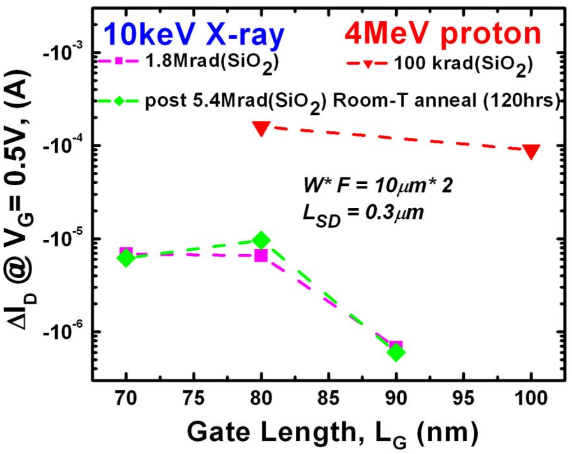

Fig. 10. Impact of 10 keV X-ray and 4 MeV proton irradiation on the saturation current.

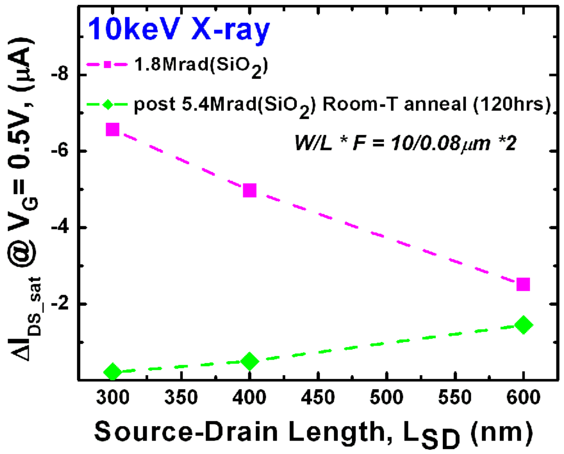

Fig. 11. Variation of the X-ray impact on saturation current ($V_G = 0.5$ V) with L_{SD}.

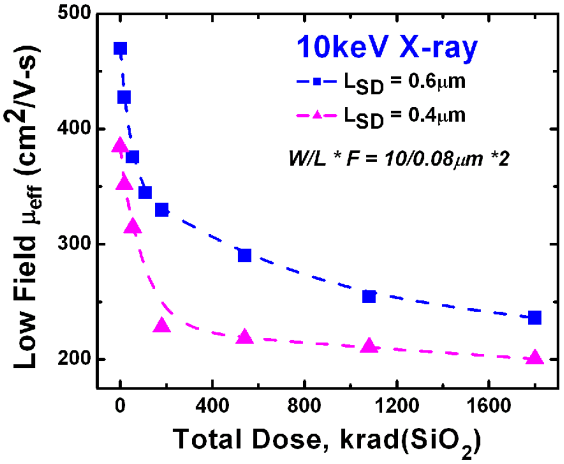

Fig. 12. Low-field mobility degradation is observed after X-ray radiation.

the mobility reduction factor of the source/drain series resistance [9]. Significant mobility degradation is observed at low total dose, saturating at higher total dose, as shown in Fig. 12.

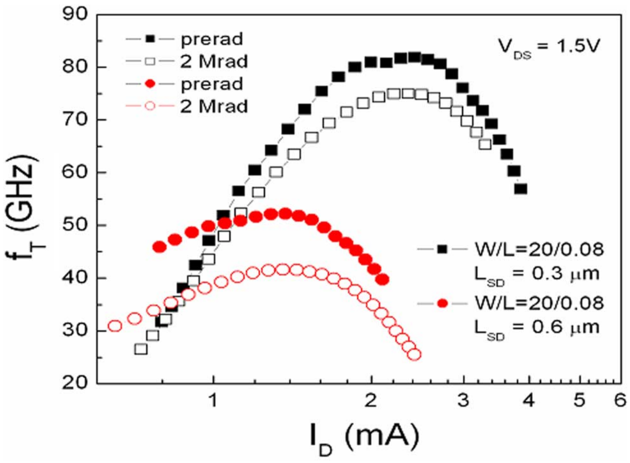

Fig. 13. Cut-off frequency degradation with 4 MeV proton passive exposure.

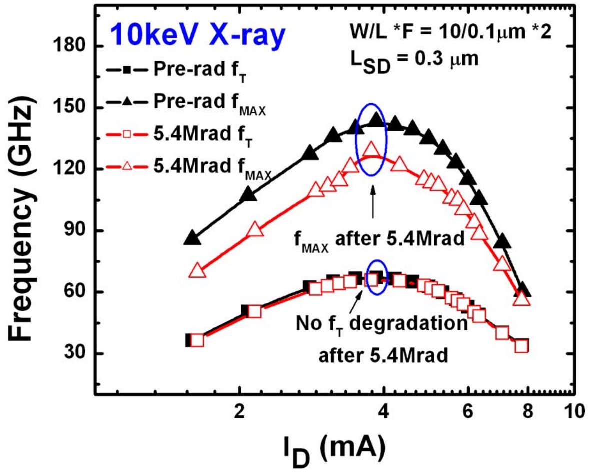

Fig. 14. Degradation in RF characteristics after 10 keV X-ray passive exposure.

B. RF Characteristics

Fig. 13 shows the low energy proton induced cut-off frequency (f_T) degradation as a function of drain current. A 2.0 Mrad(SiO_2) passive exposure was performed for devices with L_{SD} = 300 nm and 600 nm, with $(W/L) * F = (10/0.080) * 2$. Devices with an L_{SD} of 600 nm show stronger peak f_T degradation compared to those with shorter L_{SD}, suggesting that larger displacement damage in the longer L_{SD} devices results in significant transconductance degradation. X-ray induced degradation in the RF characteristics is shown in Fig. 14, after a 5.4 Mrad(SiO_2) exposure. No significant change in the peak f_T is observed, but about 10% degradation in peak f_{max} is observed. Interestingly, X-ray induced damage is also enhanced for the longer L_{SD} devices, as shown in Fig. 15. Both peak f_T and peak f_{max} degrade by about 20% and 40%, respectively, for devices with longest L_{SD} of 800 nm.

V. TCAD SIMULATIONS

2-D device simulations are performed using the Sentaurus device simulator [10]. We use a boundary description tool to define the device structure and doping. The dependence of electron affinity and bandgap of strained-Si and SiGe on the mole fraction of germanium is considered to emulate the correct band-

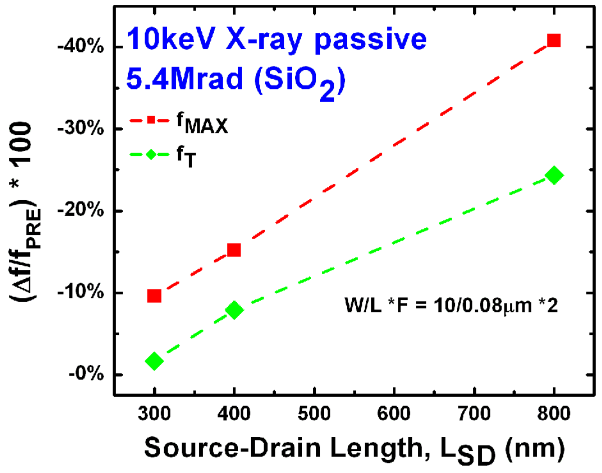

Fig. 15. Higher degradation in RF characteristics is observed for longer L_{SD} devices.

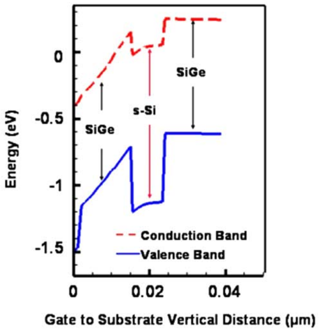

Fig. 16. Simulated band diagram of the DUT along the vertical direction (gate to substrate).

alignment for confinement of electrons. The electrons are confined in the thin strained silicon layer capped by SiGe on both sides, as shown in Fig. 16. The metal gate contact is defined as a Schottky gate with a work-function of 4.3eV to obtain reasonably good transfer characteristics from simulations. The drift-diffusion model is used for simulation of carrier transport.

A. *Displacement Damage*

Low energy proton induced displacement damage has been studied for GaN based HEMTs [11], [12]. The increase in gate current of SiGe MODFETs caused by 4 MeV low energy protons is attributed to displacement damage. Low energy protons produce higher damage in the top strained layers due to slower penetration than 63 MeV high energy protons. The displacement damage, presumably in the unrelaxed SiGe layer, degrades the confinement of the electrons in the 2-D electron gas (2DEG) strained silicon channel, as depicted in Fig. 17. The shift in CBO is attributed to the displacement damage induced strain relaxation. Simulations with a reduction in $CBO_{s-Si/SiGe}$, possibly induced by displacement damage, show an increase in I_G, as can be seen in Fig. 18. These trends are in agreement with gate current experimental data (Fig. 7).

The change in gate current (ΔI_G), especially at high drive current, increases with the lowering of the CBO. This is due to the presence of a favorable electric field for injection of electrons from the strained silicon channel into the SiGe confinement layer. As shown in Fig. 19, ΔI_G increases with reduction in $CBO_{s-Si/SiGe}$.

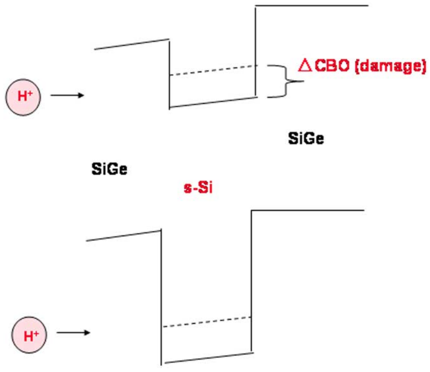

Fig. 17. Displacement damage reduces the confinement of electrons in strained-silicon conduction band. The dashed line shows the conduction band offset after strain relaxation due to displacement damage.

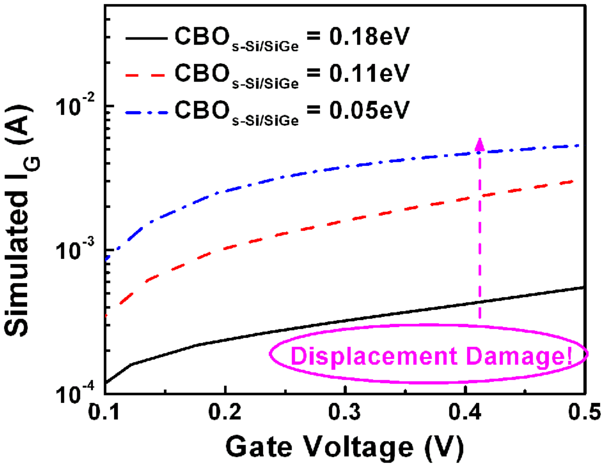

Fig. 18. Simulated gate currents with lowering of $CBO_{s-Si/SiGe}$ show similar trends with experimental data (contained in Fig. 7).

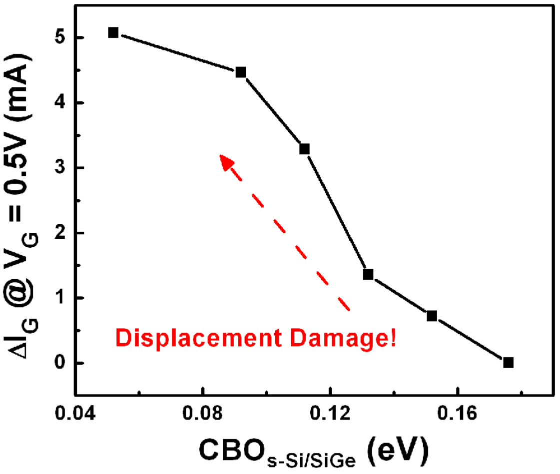

Fig. 19. ΔI_G increases with change in conduction band offsets indicating higher displacement damage.

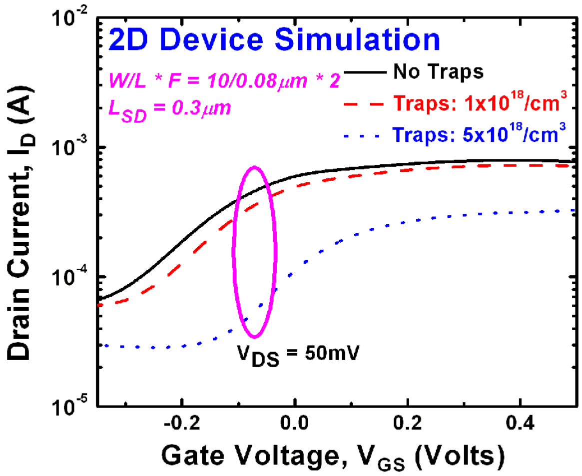

Fig. 20. Simulated transfer characteristics of n-MODFETs with bulk traps introduced inside the SiGe cap layer.

B. Role of Traps

The SiGe layer on top of the strained-silicon channel is also strained, potentially resulting in a lower activation energy for trap formation via radiation exposure. We performed device simulations with bulk traps in this unrelaxed SiGe layer to investigate the impact of radiation-induced trap formation on n-MODFET characteristics. The Shockley–Read–Hall (SRH) recombination mechanism is taken into account while analyzing the role of traps [10]. In Fig. 20, the simulated transfer characteristics with bulk traps in the unrelaxed SiGe layer show trends in agreement with experimental data for the 63 MeV proton and 10 keV X-ray irradiated devices.

These observations are also consistent with the fact that radiation damage is more L_{SD} dependent than L_G dependent. A higher L_{SD} will have more volume of unrelaxed SiGe for generation of radiation-induced bulk traps. These results can also explain the observed room temperature annealing characteristics of the post-irradiated devices, presumably due to the spontaneous annealing of traps.

VI. SUMMARY

The results from 63 MeV proton, 4 MeV proton, and 10 keV X-ray irradiation indicate that strained-Si/SiGe n-MODFETs are relatively sensitive to ionizing radiation, due to the presence of highly stained and unrelaxed heterostructures in the bulk of device. The radiation damage on both DC and RF characteristics is most strongly dependent on the device design parameter, L_{SD}. Strain relaxation and trap generation are presumably the two dominant mechanisms for the observed radiation damage in these devices. A smaller L_{SD} would reduce the radiation sensitivity of these devices. While low energy protons are able to induce strain relaxation in the heterojunctions, higher energy protons presumably increase the trap density in unrelaxed SiGe layers. However, the trap induced damage becomes appreciable at dose rates as high as 1.8 Mrad, which can be partially recovered after annealing at room temperature. Low energy protons cause maximum damage, even at low dose rates of 100 krad, due to enhanced displacement damage, which is supported by TCAD simulations.

ACKNOWLEDGMENT

The authors would like to thank IBM for their contributions to this work.

REFERENCES

[1] K. Ismail, “Si/SiGe high-speed field-effect transistors,” *IEDM Tech. Dig.*, pp. 509–512, 1995.

[2] U. Konig, M. Gluck, and G. Hock, “Si/SiGe field-effect transistors,” *J. Vac. Sci. Tech. B*, vol. 16, pp. 2609–2614, 1998.

[3] M. Enciso, F. Aniel, P. Crozat, R. Adde, M. Zeuner, A. Fox, and T. Hackarbath, “0.3 dB minimum noise figure at 2.5 GHz of 0.13 μm Si/Si$_{0.58}$Ge$_{0.42}$ n-MODFETs,” *Electron. Lett.*, vol. 37, pp. 1089–1090, 2001.

[4] S. J. Koester, R. Hammond, and J. O. Chu, “Extremely high transconductance Ge/Si$_{0.4}$Ge$_{0.6}$ p-MODFET’s grown by UHV-CVD,” *IEEE Electron Device Lett.*, vol. 21, no. 3, pp. 110–12, Mar. 2000.

[5] S. J. Koester, R. Hammond, J. O. Chu, P. M. Mooney, J. A. Ott, L. Perraud, K. A. Jenkins, C. S. Webster, I. Lagnado, and P. R. de la Houssaye, “SiGe p-MODFETs on silicon-on-sapphire substrates with 116 GHz f_{max},” *IEEE Electron Device Lett.*, vol. 22, no. 2, pp. 92–94, Feb. 2001.

[6] M. A. Listvan, P. J. Vold, and D. K. Arch, “Ionizing radiation hardness of GaAs technologies,” *IEEE Trans. Nucl. Sci*, vol. NS-34, no. 6, pp. 1664–68, Dec. 1987.

[7] B. D. Weaver, J. B. Boos, N. A. Papanicolaou, B. R. Bennett, D. Park, and R. Bass, “High radiation tolerance of InAs/AlSb high-electron-mobility transistors,” *Appl. Phys. Lett.*, vol. 87, pp. 173501–3, 2005.

[8] S. J. Koester, K. L. Saenger, J. O. Chu, Q. C. Ouyang, J. A. Ott, K. A. Jenkins, D. F. Canaperi, J. A. Tornello, C. V. Jahnes, and S. E. Steen, “Laterally scaled Si-Si$_{0.7}$ Ge$_{0.3}$ n-MODFETs with f_{max} > 200 GHz and low operating bias,” *IEEE Electron Device Lett.*, vol. 26, no. 4, pp. 178–180, Apr. 2005.

[9] G. Ghibaudo, “New method for the extraction of MOSFET parameters,” *Elec. Lett.*, vol. 24, no. 9, pp. 543–45, 1988.

[10] “Sentaurus Device Manual Version Y-2006.06,” in Synopsys Inc.

[11] B. D. White, M. Bataiev, L. J. Brillson, B. K. Choi, D. M. Fleetwood, R. D. Schrimpf, S. I. Pantelides, R. W. Dettmer, W. J. Schaff, J. G. Champlain, and A. K. Mishra, “Characterization of 1.8-MeV proton-irradiated AlGaN/GaN field-effect transistor structures by nanoscale depth-resolved luminescence spectroscopy,” *IEEE Trans. Nucl. Sci.*, vol. 49, no. 6, pp. 2695–2701, Dec. 2002.

[12] A. P. Karmarkar, B. Jun, D. M. Fleetwood, R. D. Schrimpf, R. A. Weller, B. D. White, L. J. Brillson, and U. K. Mishra, “Proton irradation effects on GaN-based high electron-mobility transistors with Si-doped AL$_x$Ga$_{1-x}$ N and thick GaN cap layers,” *IEEE Trans. Nucl. Sci*, vol. 51, no. 6, pp. 3801–06, Dec. 2004.